

Table 1 shows the numbers of iterations at convergence N_f^* , N_f^* vs the parameter k , where N_f^* is the number of iterations at convergence using the method of Yeo et al.,⁶ N_f^* is the number of iterations using the proposed method. Obviously, the proposed method has much larger region of convergence.

References

- ¹Leondes, C. T. and Paine, G., "Extensions in Quasilinearization Techniques for Optimal Control," *Journal of Optimization Theory and Applications*, Vol. 2, No. 5, 1968, pp. 316-330.
- ²Leondes, C. T. and Paine, G., "Computational Results for Extensions in Quasilinearization Techniques for Optimal Control," *Journal of Optimization Theory and Applications*, Vol. 2, No. 6, 1968, pp. 395-410.
- ³Paine, G., "The Application of the Method of Quasilinearization to the Computation of Optimal Control," Rept. 67-49, Aug. 1967, University of California, Los Angeles, Calif.
- ⁴Mukhopadhyay, B. K. and Malik, O. P., "Optimal Control of Synchronous-Machine Excitation by Quasilinearization Techniques," *Proceedings of the IEE*, Vol. 119, Jan. 1972, pp. 91-98.
- ⁵Kopp, R. and Moyer, H. G., "Trajectory Optimization Techniques," *Advances in Control Systems*, Vol. 4, Leondes, C. T., ed., Academic Press, N.Y., 1966, pp. 103-155.
- ⁶Yeo, B. P., Waldron, K. J. and Goh, B. S., "Optimal Initial Choice of Multipliers in the Quasilinearization Method for Optimal Control Problems with Bounded Controls," *International Journal of Control*, Vol. 20, No. 1, 1974, pp. 17-33.
- ⁷Yeo, B. P., "A Quasilinearization Algorithm and its Application to a Manipulator Problem," *International Journal of Control*, Vol. 20, No. 4, 1974, pp. 623-640.
- ⁸McGill, R. and Kenneth, P., "Solution of Variational Problems by Means of a Generalized Newton-Raphson Operator," *AIAA Journal*, Vol. 2, Oct. 1964, pp. 1761-1766.
- ⁹Miele, A. and Iyer, R. R., "General Technique for Solving Nonlinear Two-Point Boundary-Value Problems Via the Method of Particular Solutions," *Journal of Optimization Theory and Applications*, Vol. 5, No. 5, 1970, pp. 382-399.
- ¹⁰Bryson, A. E. and Ho, Y. C., *Applied Optimal Control*, Blaidell, Waltham, Mass., 1969.

Thermal Decomposition Studies on Ammonium Perchlorate-Based Composite Propellants

K. Kishore* and V. R. Pai Verneker†
Indian Institute of Science, Bangalore, India

Introduction

THE role of condensed-phase reactions in solid propellant combustion has long been debated. The work of Waesche and Wenograd,¹ and Sammons² in the late seventies demonstrated the importance of such reactions in the overall combustion process of a solid-propellant. Our recent studies on polystyrene (PS), ammonium perchlorate (AP) propellant system have also shed some light on the occurrence of condensed-phase reactions.^{3,4} We have shown further that the thermal decomposition of the oxidizer and the propellant in this system is correlated to its burning rate.⁵ In order to have a deeper insight into the thermal decomposition process, a quantitative analysis of the thermal changes associated with the binder, oxidizer, and the propellant is necessary. The enthalpy and kinetic estimations from the Differential Scanning

Calorimetric (DSC) thermograms of PS, AP, and PS/AP propellant form the primary objective of the present work. Another objective is to compare the activation energies (E) of the thermal decomposition of PS and AP to that of the propellant.

Experimental

PS and PS/AP propellants were prepared as described earlier.⁶ Powdered AP from Fischer Scientific Co. was used without any further purification. DSC thermograms were obtained by one of the authors (K. Kishore) at the University of Leeds, Great Britain. Isothermal and scanning thermograms were obtained on Perkin-Elmer DSC-1B Differential Scanning Calorimeter. The details of the operation of the instrument, generation of α (fraction decomposed) vs time plot, and the calculation of E from the thermograms have been described in detail in our recent publications.⁷

Results and Discussion

The DSC thermograms obtained in scanning and isothermal operations have been presented in Figs. 1 and 2. The enthalpy data for AP, PS, and AP/PS propellants obtained from the analysis of DSC thermograms are presented in Tables 1 and 2. AP endotherm starts appearing at 517 ± 2 K. The endothermic enthalpy change was calculated to be 2.39 ± 0.07 Kcal/mole which agrees well with other reported literature values.⁷

The enthalpies, for different scanning thermograms, of both low temperature exotherm (LTE) and high temperature exotherm (HTE) are given in Table 1. In order to confirm the validity of these values, isothermal runs were also carried out for LTE and the enthalpy thus calculated for isothermal runs agrees well with that from scanning runs.⁷ Assuming that the nature of decomposition is the same in LTE and HTE, we observed that 30% decomposition occurs in LTE (scanning and isotherming both operations) which is in accordance with the reported values from weight loss measurements. The total exothermic heat release of both LTE and HTE was estimated to be 278 ± 10 cal/g, which is in agreement with the earlier reported value (see Table 1) by Wenograd¹ et al.

The E values for LTE and HTE in scanning operation were calculated by the method described earlier⁷ and found to be 22.5 (21.5 in isothermal operation) and 60.5 Kcal/mole, respectively, which agree fairly well with other values using other techniques. This clearly indicates the soundness of the method used for kinetic analysis from DSC thermograms.

The propellant endotherm, appearing at 523 ± 5 K, was subjected to enthalpy estimations and was found to correspond quantitatively to the AP phase-transition endotherm (Table 1). This suggests that AP phase transformation is not affected during the casting of the propellant.

The propellant exotherm starts appearing (Fig. 1) at a later stage than the first exotherm of AP. This can be explained on the basis of a physical model⁴ which considers that AP particle or particles are surrounded by the binder. The polymer shells containing AP are closely packed in the matrix so that they make the matrix porous. According to this model, the decomposition of AP starts inside the polymer film, which further undergoes heterogeneous and homogeneous reactions with the decomposition products arising from the degradation of the inner layer of the film. This continues until finally the film is broken because of polymer degradation in its entirety, or because of build-up of the gas pressure. Polymer, being a bad thermal conductor, transfers the heat to the pan with some time lag, and that is why the actual temperature recording is shifted ahead. This also explains why the propellant exotherm finishes earlier compared to PS and AP (Fig. 1).

Since the enthalpy changes for PS, AP, and propellant (Table 1) are known, one can calculate the heat generated by the condensed-phase reactions, provided it is assumed that DSC records only solid-state reactions especially when the

Received May 22, 1975; revision received March 24, 1976.

Index categories: Thermochemistry and Chemical Kinetics; Fuels and Propellants, Properties of.

*Assistant Professor, Department of Inorganic and Physical Chemistry.

†Professor, Department of Inorganic and Physical Chemistry.

Table 1 Enthalpy data for AP, PS, and PS/AP propellants

Percentage of AP	Total heat under the exotherm cal/g	Heat of condensed-phase reactions (ΔH) _c cal/g	(ΔH) _c in cal/g calculated for 20% PS
70	620	445	297
75	562	370	396
80	492	283	283
Enthalpy for AP phase-transition endotherm			= 20.3 \pm 0.6 cal/g
Enthalpy for AP exotherms			= 278 \pm 10 cal/g
Percentage decomposition of AP (enthalpy-wise)			= 31.6 (scanning) 27.5 (isothermal)
Enthalpy for PS endotherm			= 65.5 \pm 3.3 cal/g
Enthalpy of PS/AP propellant endotherm			= 21.4 \pm 0.8 cal/g of AP

Table 2 Total exothermic enthalpy for PS/AP (70%) propellant at various temperatures in isothermal operations

Temperature ($^{\circ}$ C)	ΔH (cal/g) (uncorrected for AP and PS enthalpies)
328	400
338	420
348	430
358	500
368	530

product gases are allowed to escape constantly during the decomposition.⁷ The enthalpy (Table 1) decreases by increasing the AP content in the propellant composition. This behavior can also be explained on the basis of the model described previously. According to the model, the condensed-phase reactions will be determined by the quantity of polymer available. In Table 1, column 4, we have calculated the enthalpy change for 20% PS in different propellant compositions. The values are almost constant, showing that condensed-phase heat generation depends upon the quantity of polymer available, i.e., on propellant composition.

The enthalpy changes of the propellant in isothermal operation are given in Table 2. The quantity of heat produced increases by increasing the temperature. The values at all the given temperatures are much less than the value obtained in scanning operation. A correlation was found to exist between the temperature of decomposition and the total heat release. The value predicted by this correlation (610 cal/g) agrees well with the value of heat release for scanning operation (620

cal/g). This is surprising in view of the differences between the isothermal and the scanning techniques. No residue was found to remain in the pan after the completion of decomposition.

The isothermal results can be explained as follows. The selected temperature range for study is less than the temperature for complete decomposition in scanning run; therefore the reactions occurring at higher temperatures in scanning runs do not occur in isothermal runs which in turn give low heat production. This argument may look naive when we find that no residue remains after decomposition at all temperatures, i.e., that all the solid is decomposed. It shows that thermal decomposition is temperature sensitive, and that the nature of decomposition reactions changes with the change of temperature.⁴ This implies that the activation energy for the high temperature reactions may be different from that of the low temperature thermal decomposition of the propellant.

The propellant E values were calculated for scanning as well as isothermal exotherms. In scanning runs E was estimated at $\alpha=0.2$ and 0.8. At $\alpha=0.2$, the plot shows two slopes corresponding to $E=21$ and 54 with the break point corresponding to $1/T=1.598$. This further shows that low temperature E is 21 and high temperature E equals 54. At $\alpha=0.8$, the value is 53. The E plots for isothermal runs (using Jacobs and Kureishy method⁹) show that E at $\alpha=0.2$ has two values (21 and 51 Kcal/mole) identical to those obtained for scanning runs. The break occurs at $1/T=1.604$ which is not far off from the scanning value corresponding to 1.598. For the range $\alpha_{0.9}-\alpha_{0.2}$, the estimated value of E comes out to be 51. Thus, the composite peak of propellant gives two E values 21 and 50 to 55 Kcal/mole which agree favorably with the two E values of AP (21 and 60 Kcal/mole). This fact is also evident from the shape of propellant exotherm in both scanning and isothermal operations (Figs. 1 and 2), which clearly indicates that it is composed of two exotherms. The extension of these two exotherms will show us that the very initial decomposition ($\alpha \approx 0$ to 0.2) corresponds to the first exotherm, whereas the last portion ($\alpha \approx 0.8$ to 1) corresponds to the next. The middle part will be a mixture of the two. It may be noted that we recently have determined the E for PS decomposition by DSC as well as other isothermal techniques⁸ and found it to be 30 Kcal/mole.⁻¹ Thus, one may suggest, although the rate⁷ determining step (i.e., E) changes with temperature and/or α -value, that the rate-determining step remains the same as that in the thermal decomposition of AP, which suggests the role of AP during the thermal decomposition and combustion of propellant.

References

- Waesche, R. H. W., and Wenograd, J., "Investigation of Solid Propellant Decomposition Characteristics and Their Relation to Observed Burning Rate," ICRPG/AIAA 2nd Solid Propulsion Conference Preprint Vol., June 6-8, 1967.

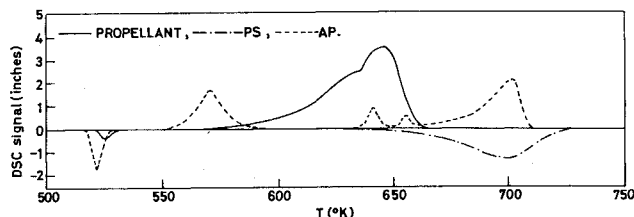


Fig. 1 Thermograms of AP, PS, and PS/AP (70%), propellant at scan speed 16 K min⁻¹. (PS, wt=2.466 mg, range=0.8 millical sec⁻¹; AP, wt=1.7216 mg, range=16 millical sec⁻¹; propellant, wt=1.392 mg, range=16 millical sec⁻¹).

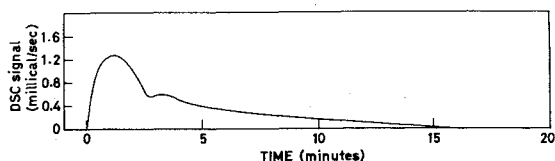


Fig. 2 Thermogram for isothermal decomposition of PS/AP (70%) propellant at 611 K. (Wt=0.889 mg).

²Sammons, G. D., "Study of the Thermal Behaviour of Solid-Propellants by Differential Scanning Calorimetry," *Analytical Chemistry*, Plenum Press, New York, 1968, pp. 305-311.

³Kishore, K., Pai Verneker, V. R., and Nair, M. N. R., "Condensed-Phase Reactions in Solid Propellant Combustion," *AIAA Journal*, Vol. 13, Sept. 1975, pp. 1,240-1,242.

⁴Pai Verneker, V. R., Kishore, K. and Nair, M. N. R., "Importance of Condensed-Phase Reactions in Solid-Propellant Combustion," Paper No. 75-1202, AIAA/SAE 11th Propulsion Conference, Anaheim, Calif., Sept. 29-Oct. 1, 1975.

⁵Pai Verneker, V. R., Kishore, K. and Mohan, V. K., "Correlation between Combustion and Decomposition of Solid-Propellants," *AIAA Journal*, Vol. 13, Oct. 1975, pp. 1415-1416.

⁶Rastogi, R. P., Kishore, K., and Singh, G., "Combustion of Polystyrene and Styrene-Oxygen Copolymer/ NH_4ClO_4 Propellants," *AIAA Journal*, Vol. 12, Jan. 1974, pp. 9-10.

⁷Kishore, K., Pai Verneker, V. R., and Mohan, V. K., "Differential Scanning Calorimetric Studies on the Thermal Decomposition of Ammonium Perchlorate," *Thermochimica Acta*, Vol. 13, 1975, pp. 277-292.

⁸Kishore, K., Pai Verneker, V. R. and Nair, M. N. R., "Thermal Degradation of Polystyrene," *Journal of Applied Polymer Science*, (In press).

⁹Jacobs, P. W. M. and Kuveisky, A. R. T., "Kinetics of Thermal Decomposition of Podium Azide," *Journal of the Chemical Society*, 1964, pp. 4718-4723.

Compressible Laminar Boundary Layers with Large Acceleration and Cooling

Lloyd H. Back* and Robert F. Cuffel†
Jet Propulsion Lab., California Institute of Technology, Pasadena, Calif.

Nomenclature

a_{T_0}	= sound speed at reservoir condition
c_D	= mass flow coefficient
c_f	= friction coefficient, $(c_f/2) = (\tau_w/\rho_e u_e^2)$
D	= diameter
f'	= dimensionless velocity, u/u_e
f''_w	= gradient at surface in transformed coordinates
F	= correlation function, Eq. (3)
g_w	= surface to total gas enthalpy, H_w/H_{T_0}
G	= dimensionless total enthalpy difference, Ref. 5
H	= static enthalpy
H_T	= total enthalpy, $H + u^2/2$
M	= Mach number
r_w	= body or channel radius
r_{th}	= throat radius
r_c	= throat radius of curvature
$Re_{\bar{\theta}}$	= momentum thickness Reynolds number, $\rho_e u_e \bar{\theta}/\mu_e$
$Re_{D_{th}}$	= throat Reynolds number, $(\rho_e u_e D/\mu_e)_{th}$
T	= temperature
u	= velocity component parallel to surface
x	= distance along surface
y	= distance normal to wall
z	= axial distance
β	= acceleration parameter in transformed coordinates, Ref. 5

Received June 30, 1975; revision received December 14, 1975. This work presents the results of one phase of research carried out in the Propulsion and Materials Research Section of the Jet Propulsion Laboratory, California Institute of Technology, under Contract NAS7-100, sponsored by the National Aeronautics and Space Administration.

Index categories: Boundary Layers and Convective Heat Transfer; Nozzle and Channel Flow.

*Member Technical Staff, Associate Fellow AIAA.

†Member Technical Staff, Member AIAA.

$\beta\theta_t^2$

= acceleration parameter, Eq. (3)

γ

= specific heat ratio

δ^*

= boundary-layer thickness, $[1 - (\rho u/\rho_e u_e)]$

δ^*

= displacement thickness,

$$r_w^j \delta^* = \delta^* (r_w - \delta^* \cos \sigma/2)^j$$

$$= \int_0^\infty [(1 - (\rho u/\rho_e u_e))] (r_w - y \cos \sigma)^j dy$$

δ_t^*

= transformed displacement thickness, Eq. (5)

η

= dimensionless transformed coordinate normal to surface

$\bar{\theta}$

= momentum thickness,

$$r_w^j \bar{\theta} = \theta (r_w - \theta \cos \sigma/2)^j$$

$$= \int_0^\infty (\rho u/\rho_e u_e) (1 - u/u_e) (r_w - y \cos \sigma)^j dy$$

θ_t

= transformed momentum thickness, Eq. (5)

μ

= viscosity

ν

= kinematic viscosity

ρ

= density

σ

= angle between wall and axis

τ_w

= surface shear stress

Subscripts

e

= condition at freestream edge of boundary layer

o

= reservoir condition

T

= stagnation condition

th

= throat condition

w

= surface condition

Introduction

THIS Note is concerned with extending an approximate prediction method involving the integral form of the momentum equation¹ to deduce the flow quantities of interest when compressibility effects become important and heat transfer may occur. The approximate method is applicable to a two-dimensional, laminar boundary layer on an im-

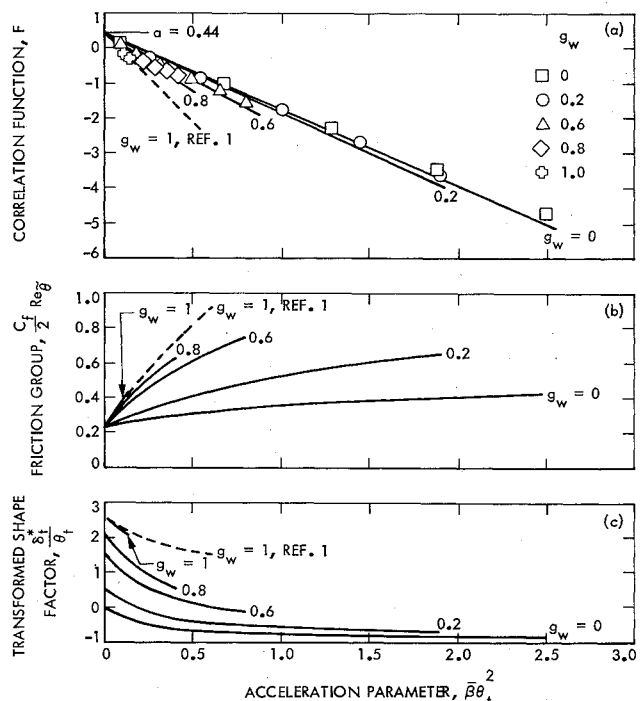


Fig. 1 Variation of the correlation function F , friction group $c_f/2 Re_{\bar{\theta}}$, and transformed shape factor δ_t^*/θ_t with acceleration parameter $\beta\theta_t^2$ and surface-to-total gas enthalpy parameter g_w .